Generalized Dicke Nonequilibrium Dynamics in Trapped Ions

Sam Genway,[1] Weibin Li,[1] Cenap Ates,[1] Benjamin P. Lanyon,[2,3] and Igor Lesanovsky[1]
[1]*School of Physics and Astronomy, The University of Nottingham, Nottingham NG7 2RD, United Kingdom*
[2]*Institut für Quantenoptik und Quanteninformation, Österreichische Akademie der Wissenschaften, Technikerstr. 21A, 6020 Innsbruck, Austria*
[3]*Institut für Experimentalphysik, Universität Innsbruck,Technikerstr. 25, 6020 Innsbruck, Austria*
(Received 6 August 2013; published 15 January 2014)

We explore trapped ions as a setting to investigate nonequilibrium phases in a generalized Dicke model of dissipative spins coupled to phonon modes. We find a rich dynamical phase diagram including superradiantlike regimes, dynamical phase coexistence, and phonon-lasing behavior. A particular advantage of trapped ions is that these phases and transitions among them can be probed *in situ* through fluorescence. We demonstrate that the main physical insights are captured by a minimal model and consider an experimental realization with Ca^+ ions trapped in a linear Paul trap with a dressing scheme to create effective two-level systems with a tunable dissipation rate.

DOI: 10.1103/PhysRevLett.112.023603 PACS numbers: 42.50.Nn, 03.65.Yz, 64.60.an

The exploration and the understanding of the equilibrium and in particular the nonequilibrium behavior [1–6] of quantum many-body systems is of great current interest. Due to recent experimental advances trapped ions have become a very flexible platform to approach this challenging problem [7–9]. In particular, spin systems [10,11] have been investigated with both a few [12] and several hundred ions [13,14] and a variety of phenomena such as the emergence of interesting quantum phases [8,10,15,16], the dynamical formation of defects [17,18], and the role of frustration [19,20] have been explored. This flexibility is rooted in the fact that the coherent coupling between electronic states (forming effective spin degrees of freedom) and the vibrations of an ion crystal can be precisely controlled.

Such coupling between spins and oscillator degrees of freedom in general leads to intriguing many-body effects. A paradigmatic example is seen in the Dicke model (DM) [21], originally proposed to study superradiance in quantum electrodynamics [22–24]. The DM features a continuous quantum phase transition (QPT) at critical coupling between the spins and oscillator degrees of freedom. The QPT connects a "normal" phase, where the oscillator is in its ground state, to a "superradiant" phase with a displaced oscillator. Due to the coupling of the oscillator to the spins, this QPT becomes equally manifest in the polarization of the spins. Dicke physics gives insights into a variety of phenomena such as quantum chaos [25] and the physics of spin glasses [26]. This versatility has ushered renewed interest in exploring both statics and dynamics [27–30]. In particular much effort is currently put into experimentally realizing Dicke systems out of equilibrium —a recent example is the investigation of the nonequilibrium dynamics of superfluid cold atomic gases in optical cavities [31,32].

In this work we show that a generalized version of the DM— where dissipation is introduced on the individual spins— captures the nonequilibrium physics of a crystal of laser-driven trapped ions. Analogous to the QPT in

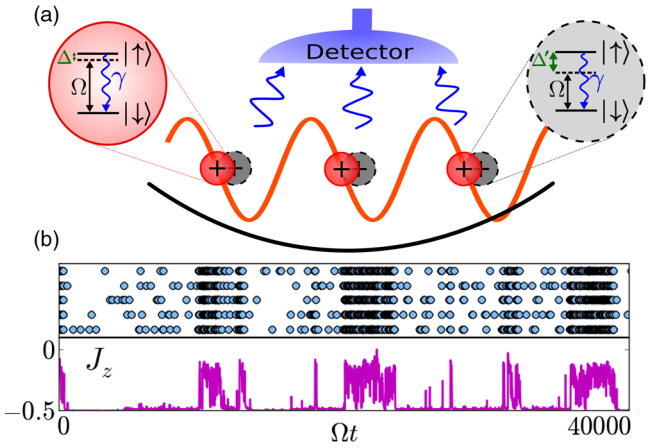

FIG. 1: (color online). (a) Schematic diagram of a one-dimensional ion crystal in different dynamical phases. Shown are two electronic states of each ion representing states $|\downarrow\rangle$ and $|\uparrow\rangle$ of a fictitious spin. Transitions between electronic (spin) states are driven by a laser with Rabi frequency Ω and detuning Δ. The state $|\uparrow\rangle$ relaxes to $|\downarrow\rangle$ at a spontaneous decay rate γ. Photons emitted in this process are detected with spatial and temporal resolution. Electronic states couple to motional degrees of freedom through a far-detuned standing-wave laser field. Upon increasing this coupling there is a dynamical phase transition where the ions become displaced in the trap (dashed circles). The displacement leads to a large effective detuning Δ' such that the electronic state $|\uparrow\rangle$ is rarely populated and the fluorescence signal is greatly reduced. (b) Regions in parameter space where both dynamical phases coexist are revealed by an intermittent fluorescence signal. The data shown correspond to a QJMC trajectory of five ions and display the times and positions of photon emissions (top) and the spin z-polarization J_z (bottom).

the closed-system DM, we identify dynamical phase transitions (DPTs) associated with singular changes in steady states of the system in the thermodynamic limit. The dynamical phases of this system and the associated DPTs are directly linked to the time-resolved fluorescence signal from photon emissions of the ions [5]. This allows for the in situ probing of collective dynamics resulting from a competition between the coupling of spins to vibrational degrees of freedom (phonons in the ion trap) [33,34] and tuneable spin dissipation [see Fig. 1(a)]. The dynamical phase diagram of the generalized DM includes nonequilibrium steady states related to the traditional normal and superradiant phases as well as a phase coexistence region. These phases become manifest in time-resolved fluorescence measurements as bright and dark regions, with phase coexistence resulting in temporal intermittency, as illustrated in Fig. 1(b). In contrast with the QPT of the conventional DM, the DPT of the generalized DM is first order and the phase diagram includes a new phase where phonon lasing occurs.

In order to obtain a basic understanding of the physics of the driven trapped ion system, we begin by studying a minimal model of N ions coupled to only a single phonon mode. Later, we generalize this to the situation found in an ion crystal formed by Ca^+ with many modes. The minimal model is described by the Hamiltonian

$$H = \Omega \sum_{i=1}^{N} S_i^x + \Delta \sum_{i=1}^{N} S_i^z + V \sum_{i=1}^{N} S_i^z (a + a^\dagger) + \omega a^\dagger a. \tag{1}$$

Here, S_i^x, S_i^z are spin operators for the internal states of the ion at position i in the trap [as in Fig. 1(a)]. a ($a^\dagger$) is the bosonic annihilation (creation) operator for the axial center-of-mass phonon mode, with frequency ω, such that a nonzero $\langle a + a^\dagger \rangle$ corresponds to a displacement of all ions along the trap. The ions are driven with Rabi frequency Ω and detuning Δ. An electronic-state-dependent force of strength V can be constructed [34,35] with a far-detuned standing-wave laser field with the ions positioned at nodes. At $\Delta = 0$, Eq. (1) is the DM Hamiltonian, with a continuous QPT associated with a discrete symmetry breaking when $NV^2 = \Omega\omega$. Without dissipation, finite Δ smoothes the QPT into a crossover [36].

The effective decay of the spins [see Fig. 1(a)] with rate γ is captured by the dissipator $D(\rho) = \gamma \sum_i (S_i^- \rho S_i^+ - (1/2)\{S_i^+ S_i^-, \rho\})$. The evolution of the density matrix is thus governed by $\dot{\rho} = \mathcal{W}(\rho) = -i[H, \rho] + D(\rho)$. In the following, we consider the case of trapping frequency $\omega = N\Omega$, as this scaling renders the phase boundaries N independent. We employ a mean-field (MF) approach to study semiclassical dynamics and complement this with quantum-jump Monte Carlo (QJMC) simulations [37], which illustrate what would be seen in experiment.

We find MF equations for the expectation values $A = \langle a \rangle$ and the macroscopic spin polarization $J_k = \langle (1/N) \sum_i S_i^k \rangle$, for $k = x, y, z$:

$$\begin{aligned} \dot{A} &= -i\omega A - iVJ_z N, \\ \dot{J}_x &= -\frac{\gamma}{2} J_x - VJ_y (A + A^*) - \Delta J_y, \\ \dot{J}_y &= -\frac{\gamma}{2} J_y - \Omega J_z + VJ_x (A + A^*) + \Delta J_x, \\ \dot{J}_z &= -\gamma \left(J_z + \frac{1}{2} \right) + \Omega J_y. \end{aligned} \tag{2}$$

Although information about fluctuations has been lost by replacing expectation values of products of the form $\langle (1/N) \sum_i S_i^k a \rangle$ by products of expectation values $J_k A$, the equations still capture approximate average dynamics. These equations reveal two main differences from the traditional DM [25] and the DM with dissipation only in the oscillator degrees of freedom [28]. First, the length of the macroscopic spin J^2 is not conserved so that fixed points [38] traditionally associated with normal (zero oscillator displacement) and superradiant (large oscillator displacement) phases are different in nature. Second, there is no spontaneous symmetry breaking between states with opposite J_z and oscillator displacement $X = (A + A^*)/2$ as the dissipation acting on the individual spins always selects the macroscopic spin-down state over a state with positive J_z.

Our aim is to identify steady states of the quantum problem with the stable fixed points of the MF equations (2). Figure 2(a) shows the dynamical phase diagram found from these fixed points for $\Delta = 0$ as a function of V and γ. The insets show examples of time- and space-resolved fluorescence measurements for five ions obtained by QJMC simulations of the full model. The fluorescence signals are clearly linked to the various phases. In particular, we see a "bright phase" (B) corresponding to the state with vanishing oscillator displacement X and a "dark phase" (D) when $X > 0$. In the bright phase, the effects of driving and dissipation dominate and, in our MF analysis, the stable fixed point lies far within the Bloch sphere. In the dark phase, the coupling of spins to the phonon mode leads to an oscillator displacement a large effective detuning [see Fig. 1(a)], given by $\Delta' = \Delta + 2VX$ in the MF analysis. This suppresses the driving and dissipation leading to a large spin polarization.

In the limit $\gamma \to 0^+$ we find a simple expression for the critical coupling V_c, above which the D fixed point is stable in the thermodynamic limit: $V_c = (2^{1/2}\Omega\omega/N)^{1/2}$, for general trapping frequency ω. This value differs from the nondissipative DM as does the nature of the transition itself. It is first order and associated with a region of phase coexistence ($B + D$), which occurs at finite $\gamma \lesssim 0.5\Omega$, beyond V_c. In the fluorescence records this phase coexistence shows up as a pronounced intermittency characterised by a switching between bright and dark periods. The effect is strongly

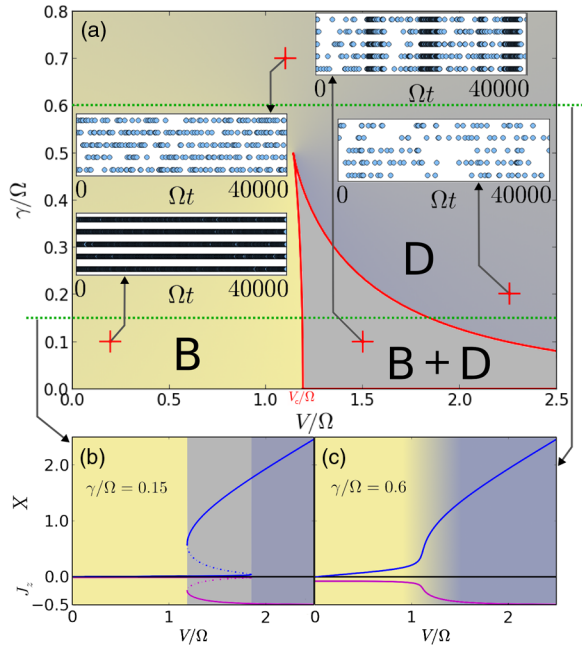

FIG. 2: (color online). Dynamical phase diagram for $\Delta = 0$. (a) The MF phase diagram found from the fixed-point analysis of Eqs. (2) as a function of the coupling V and inverse lifetime γ for $\omega/N = \Omega$. Shown are the bright (B) and dark (D) regimes and a region of phase coexistence ($B + D$). The phases are distinguished by both spin-polarization and ion-displacement order parameters. Inset: QJMC simulations for a five-ion system at parameter values V, γ as indicated. Shown are quantum trajectories in the steady state, with markers indicating the times at which photon emissions occur for each of the five ions along the ordinate axes. (b,c) Plots of the polarization J_z and phonon displacement $X = (A + A^*)/2$ at fixed points as a function of V/Ω for $\gamma/\Omega = 0.15$ (b) and $\gamma/\Omega = 0.6$ (c). Solid lines indicate stable fixed points.

dependent on system size, with the existence of longer bright and dark periods at larger N (see the Supplemental Material [39]). While the steady states are classical in nature, the noise which causes switching is of quantum origin as it arises from the spin dissipation. When crossing the DPT, there is a sharp change in J_z and the displacement of the ions in the trap, associated with the emergence of a new stable fixed point of the MF equations [see Fig. 2(b)]. So we see that a structural transition in the ion positions is associated with a DPT in the fluorescence in the thermodynamic limit [5]. At large $\gamma \sim \Omega$, as shown in Fig. 2 (c), the DPT becomes a crossover where the fixed point moves continuously from bright to dark phases with increasing V. We note that intermittency in fluorescence signals is not seen in this crossover region.

Surprisingly, in contrast with the closed-system DM QPT [36], a finite detuning Δ does not destroy the DPTs shown in Fig. 3. For small $\Delta > 0$, MF steady states remain qualitatively unchanged and quantitatively very similar. One might imagine that a negative detuning would compete with spin dissipation to take the system towards a steady state with a large and positive J_z at large V, as in the closed system. However, as shown in Fig. 3, for $\Delta < 0$ we find that the fixed points at small γ and V actually become unstable at Hopf bifurcations [38] and, in these regimes, limit-cycle oscillations in the phonon dynamics are found at long times. This phenomenon has been observed in trapped ions and is known as phonon lasing [40]. These regions, labeled PL, are shown in Fig. 3, where we also plot two example semiclassical trajectories towards the dark fixed point and the limit cycle. While it appears unphysical that limit cycles persist down to $V = 0$, this feature is destroyed by any finite phonon dissipation. Such dissipation inevitably occurs in trapped-ion experiments. We introduce a finite dissipation rate $\kappa/N \ll \gamma$ on the motional degrees of freedom by replacing $\omega \to \omega - i\kappa$ in the MF equations (2). This changes all dynamical phase boundaries negligibly except for the phonon lasing regime, which becomes suppressed at small V with finite κ (see Fig. 3).

So far we have only included the center-of-mass phonon mode in our considerations. In a trapped-ion crystal, an electronic-state-dependent force on the ions constructed with a far-detuned standing-wave laser field will couple the electronic states to all phonon modes. We explore the role of the higher-frequency modes by extending the simple model (1). The phonon modes have frequencies ω_m, for $m = 1$ to N, and couple to the spins via the coupling Hamiltonian $\sum_{im} V_{im} S_i^z (a_m + a_m^\dagger)$. Here $a_m^\dagger$ is the creation operator for mode m. The coupling matrix

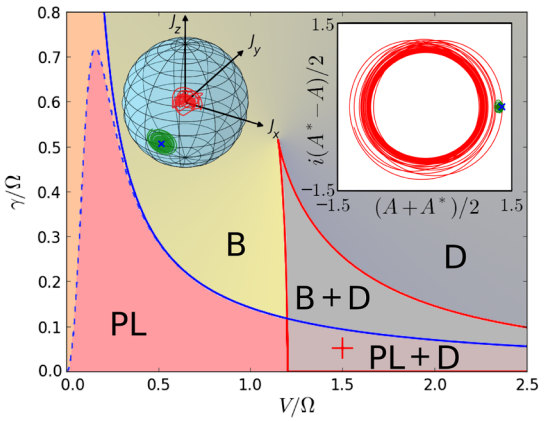

FIG. 3: (color online). Dynamical phase diagram for $\Delta = -0.01\ \Omega$ with all other parameters as in Fig. 2. In addition to the bright (B), dark (D), and coexistence ($B + D$) regimes, points where the bright fixed point disappears at a Hopf bifurcation are shown for $\kappa = 0$ (solid blue line) and $\kappa/N = 10^{-4}\ \Omega$ (dashed blue line). Beyond these birfurcations, limit-cycle solutions corresponding to phonon lasing (PL) exist. Beyond the critical coupling there exists a new region ($PL + D$) where the dark fixed point is stable but the bright fixed point bifurcates. The parameters indicated by "+" are used for the insets. Shown inset are plots of the MF dynamics with different initial conditions showing the Bloch sphere and oscillator phase plane for limit-cycle (red) and fixed-point (green) steady states. The dark fixed point is labeled "×."

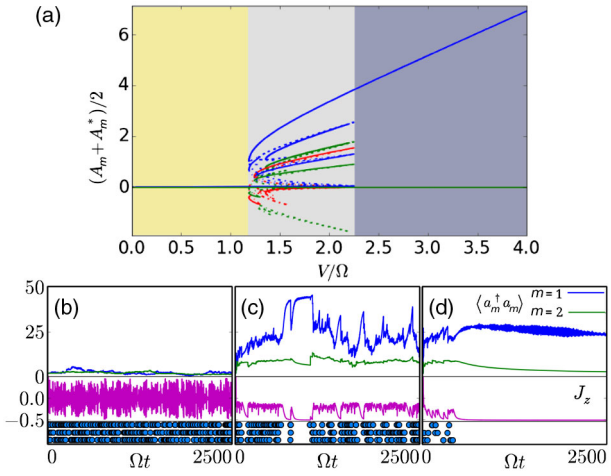

FIG. 4: (color online). (a) Oscillator displacements at the fixed points of the three-spin, three-oscillator model as a function of the coupling V, for $\gamma = 0.1$ and $\kappa = \Delta = 0$. Regions where the fixed points are stable are shown with solid lines with all other fixed-point classifications plotted with dashed lines. Plotted are the center-of-mass mode with frequency ω_1 (blue), and the modes (see the Supplemental Material [39]) with frequencies ω_2 (green) and ω_3 (red). (b,c,d) Sample trajectories with phonon modes $m = 1$ and 2 included showing the occupation of the two included phonon modes (top), the polarization J_z (middle), and photon emissions (bottom) of a three-ion simulation for $V = 0.1$ (b), $V = 1.5$ (c), and $V = 3.5$ (d).

elements V_{im} are proportional to the normal-mode displacement vectors of the ions [33], so that all vibrational modes with frequencies above $\omega_1 = \omega$ have a heterogeneous phonon-spin coupling. Thus, different spins and phonon modes have different MF equations and Eqs. (2) are replaced with $4N$ equations.

To be specific, let us study in detail the case of a three-ion system and analyze the fixed points of the 12 coupled equations associated with this three-spin, three-oscillator model (see the Supplemental Material [39]). We find the stable fixed points in the single-mode model (2) are also stable fixed points of many-mode dynamics (see the Supplemental Material [39]). In addition to these steady states, in the coexistence region we find a family of additional fixed points, which we illustrate in Fig. 4(a). None of these additional steady states exists at large $V \gtrsim 2.3\Omega$. In Figs. 4(b)–4(d) we confirm these inferences by performing QJMC simulations for three trapped ions, including both the center-of-mass mode and, additionally, the next mode with frequency ω_2. Although the additional phonon mode we include becomes populated close to the DPT, we still observe temporal intermittency in the photon emission rate, associated with a switching between states with different J_z. Crucially, far into the bright and dark regimes, our prediction that higher-frequency modes will not play a role is confirmed with QJMC simulations.

We now check that the ion recoil due to the fluorescence, which allows us to probe dynamical phases, does not itself significantly change the dynamics. When ion recoil is included in the model, the full Liouvillian for the spontaneous emission process couples the spatial and internal ion degrees of freedom. For a single phonon mode, the Lindblad operators $L_i(x) = \sqrt{\gamma W(x)} e^{i\eta(a+a^\dagger)x} S_i^-$ form a continuum with $-1 \le x \le 1$. $W(x) = 3/4(1+x^2)$ reflects the angular distribution for a dipole transition and η is the Lamb-Dicke parameter [41]. Repeating our fluorescence-signal simulations in Fig. 2 with the full Liouvillian associated with spontaneous emission we find the collective quantum-jump behavior qualitatively the same with $\eta = 1/10$. In this Lamb-Dicke regime, if we expand the Liouvillian up to second order in η as in Ref. [41], the semiclassical Eqs. (2) are unchanged.

Finally, let us show how to control the decay rate γ which is essential for mapping out the phase diagram. This can be tuned in a Ca^+-ion crystal using a simple dressing scheme [42]. Effective two-level systems (TLSs) can be created from the ions' $|4S_{1/2}\rangle$, $|4P_{3/2}\rangle$, and $|3D_{5/2}\rangle$ states (see Fig. 5). We employ a strong dressing laser, with Rabi frequency Ω_D and detuning Δ_D, between the $|3D_{5/2}\rangle$ and $|4P_{3/2}\rangle$ states. Projecting out the fast dynamics associated with the state $|4P_{3/2}\rangle$ using the method of adiabatic elimination [43], we find effective driven and dissipative TLSs with an effective dissipation rate γ, which can be adjusted by tuning Ω_D. The effective detuning Δ can be removed completely by an appropriate detuning δ of the driving laser with Rabi frequency Ω. We find effective TLS parameters $\gamma = [(\Gamma_1+\Gamma_2)\Omega_D^2]/[(\Gamma_1+\Gamma_2)^2 + 4\Delta_D^2]$ and $\Delta = \delta - \Delta_D\gamma/[(\Gamma_1+\Gamma_2)]$. For Ca^+, $\Gamma_1^{-1} = 7.4\times10^{-9}$ s and $\Gamma_2^{-1} = 101\times10^{-9}$ s so that for $\Omega_D = 10$ MHz and $\Delta_D = 300$ MHz with $\Omega = 0.2$ MHz and $\delta = 79$ kHz we have an effective TLS with $\gamma/\Omega \simeq 0.19$ and $\Delta \simeq 0$. The system reaches an effective TLS steady state on short time scales $\lesssim 150$ μs. Therefore, the dynamical phases discussed in this work are observable on experimental time scales, even though the fluorescence rates are significantly lower than when driving on a dipole-allowed transition [44,45]. The full counting statistics for the fluorescence can be inferred from repeated experiments.

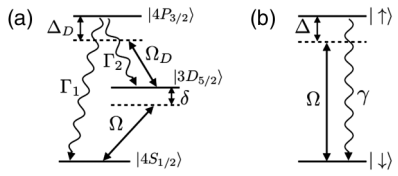

FIG. 5: (a) Level structure of Ca^+ ions driven by dressing laser of Rabi frequency Ω_D with detuning Δ_D, with decay rates Γ_1 and Γ_2 shown. The driven transition has $\Omega, \delta \ll \Omega_D \ll \Delta_D, \Gamma_1, \Gamma_2$. (b) The effective two-level scheme after projecting out the fast degrees of freedom, with unmodified Rabi frequency Ω, effective detuning and decay rate Δ, and γ. The scheme provides the states $|\downarrow\rangle$ and $|\uparrow\rangle$ which derive from $|4S_{1/2}\rangle$ and $|3D_{5/3}\rangle$ dressed with $|4P_{3/2}\rangle$.

We wish to thank Tobias Brandes, Andrew Armour, and Clive Emary for useful discussions. This work was supported by The Leverhulme Trust under Grant No. F/00114/BG, EPSRC and the ERA-NET CHIST-ERA (R-ION Consortium). W. L. is supported through the Nottingham Research Fellowship by the University of Nottingham. C. A. acknowledges funding through a Marie Curie Fellowship. B. P. L. acknowledges support from the Austrian Research Fund under project number P25354-N20. The research leading to these results has received funding from the European Research Council under the European Union's Seventh Framework Programme (FP/2007-2013) / ERC Grant Agreement no. 335266 (ESCQUMA).

[1] C. Kollath, A. M. Läuchli, and E. Altman, Phys. Rev. Lett. **98**, 180601 (2007).
[2] S. Diehl, A. Tomadin, A. Micheli, R. Fazio, and P. Zoller, Phys. Rev. Lett. **105**, 015702 (2010).
[3] A. Tomadin, S. Diehl, and P. Zoller, Phys. Rev. A **83**, 013611 (2011).
[4] E. M. Kessler, S. Yelin, M. D. Lukin, J. I. Cirac, and G. Giedke, Phys. Rev. Lett. **104**, 143601 (2010); E. M. Kessler, G. Giedke, A. Imamoglu, S. F. Yelin, M. D. Lukin, and J. I. Cirac, Phys. Rev. A **86**, 012116 (2012).
[5] C. Ates, B. Olmos, J. P. Garrahan, and I. Lesanovsky, Phys. Rev. A **85**, 043620 (2012).
[6] S. Genway, J. P. Garrahan, I. Lesanovsky, and A. D. Armour, Phys. Rev. E **85**, 051122 (2012); J. M. Hickey, S. Genway, I. Lesanovsky, and J. P. Garrahan, Phys. Rev. B **87**, 184303 (2013).
[7] P. Schindler, M. Muller, D. Nigg, J. T. Barreiro, E. A. Martinez, M. Hennrich, T. Monz, S. Diehl, P. Zoller, and R. Blatt, Nat. Phys. **9**, 361 (2013).
[8] C. Schneider, D. Porras, and T. Schaetz, Rep. Prog. Phys. **75**, 024401 (2012).
[9] M. Johanning, A. F. Varn, and C. Wunderlich, J. Phys. B **42**, 154009 (2009).
[10] D. Porras and J. I. Cirac, Phys. Rev. Lett. **92**, 207901 (2004).
[11] X.-L. Deng, D. Porras, and J. I. Cirac, Phys. Rev. A **72**, 063407 (2005).
[12] K. Kim, M.-S. Chang, R. Islam, S. Korenblit, L.-M. Duan, and C. Monroe, Phys. Rev. Lett. **103**, 120502 (2009).
[13] K. Kim, S. Korenblit, R. Islam, E. E. Edwards, M.-S. Chang, C. Noh, H. Carmichael, G.-D. Lin, L.-M. Duan, C. C. J. Wang, J. K. Freericks, and C. Monroe, New J. Phys. **13**, 105003 (2011).
[14] J. W. Britton, B. C. Sawyer, A. C. Keith, C. C. J. Wang, J. K. Freericks, H. Uys, M. J. Biercuk, and J. J. Bollinger, Nature (London) **484**, 489 (2012).
[15] A. Friedenauer, H. Schmitz, J. T. Glueckert, D. Porras, and T. Schätz, Nat. Phys. **4**, 757 (2008).
[16] R. Islam, E. E. Edwards, K. Kim, S. Korenblit, C. Noh, H. Carmichael, G.-D. Lin, L. M. Duan, C.-C. J. Wang, J. K. Freericks, and C. Monroe, Nat. Commun. **2**, 377 (2011).
[17] A. del Campo, G. De Chiara, G. Morigi, M. B. Plenio, and A. Retzker, Phys. Rev. Lett. **105**, 075701 (2010).
[18] G. D. Chiara, A. del Campo, G. Morigi, M. B. Plenio, and A. Retzker, New J. Phys. **12**, 115003 (2010).
[19] K. Kim, M. S. Chang, S. Korenblit, R. Islam, E. E. Edwards, J. K. Freericks, G. D. Lin, L. M. Duan, and C. Monroe, Nature (London) **465**, 590 (2010).
[20] A. Bermudez, J. Almeida, F. Schmidt-Kaler, A. Retzker, and M. B. Plenio, Phys. Rev. Lett. **107**, 207209 (2011).
[21] B. M. Garraway, Phil. Trans. R. Soc. A **369**, 1137 (2011).
[22] R. H. Dicke, Phys. Rev. **93**, 99 (1954).
[23] K. Hepp and E. H. Lieb, Ann. Phys. (N.Y.) **76**, 360 (1973).
[24] Y. K. Wang and F. T. Hioe, Phys. Rev. A **7**, 831 (1973).
[25] C. Emary and T. Brandes, Phys. Rev. Lett. **90**, 044101 (2003); Phys. Rev. E **67**, 066203 (2003); N. Lambert, C. Emary, and T. Brandes, Phys. Rev. Lett. **92**, 073602 (2004).
[26] P. Strack and S. Sachdev, Phys. Rev. Lett. **107**, 277202 (2011).
[27] V. M. Bastidas, C. Emary, B. Regler, and T. Brandes, Phys. Rev. Lett. **108**, 043003 (2012).
[28] F. Dimer, B. Estienne, A. S. Parkins, and H. J. Carmichael, Phys. Rev. A **75**, 013804 (2007).
[29] J. Keeling, M. J. Bhaseen, and B. D. Simons, Phys. Rev. Lett. **105**, 043001 (2010); M. J. Bhaseen, J. Mayoh, B. D. Simons, and J. Keeling, Phys. Rev. A **85**, 013817 (2012).
[30] W. Kopylov, C. Emary, and T. Brandes, Phys. Rev. A **87**, 043840 (2013).
[31] K. Baumann, C. Guerlin, F. Brennecke, and T. Esslinger, Nature (London) **464**, 1301 (2010).
[32] K. Baumann, R. Mottl, F. Brennecke, and T. Esslinger, Phys. Rev. Lett. **107**, 140402 (2011).
[33] D. James, Appl. Phys. B **66**, 181 (1998).
[34] P. J. Lee, K.-A. Brickman, L. Deslauriers, P. C. Haljan, L.-M. Duan, and C. Monroe, J. Opt. B **7**, S371 (2005).
[35] J. J. García-Ripoll, P. Zoller, and J. I. Cirac, Phys. Rev. A **71**, 062309 (2005).
[36] C. Emary and T. Brandes, Phys. Rev. A **69**, 053804 (2004).
[37] J. Johansson, P. Nation, and F. Nori, Comput. Phys. Commun. **183**, 1760 (2012); Comput. Phys. Commun. **184**, 1234 (2013).
[38] S. H. Strogatz, *Nonlinear Dynamics and Chaos: With Applications to Physics, Biology, Chemistry, and Engineering (Studies in Nonlinearity)* (Perseus Books Group, Cambridge, MA, 1994), 1st ed.
[39] See Supplemental Material at http://link.aps.org/supplemental/10.1103/PhysRevLett.112.023603 for a brief discussion of system size and the treatment of multiple phonon modes.
[40] K. Vahala, M. Herrmann, S. Knünz, V. Batteiger, G. Saathoff, T. Hänsch, and T. Udem, Nat. Phys. **5**, 682 (2009).
[41] J. I. Cirac, R. Blatt, P. Zoller, and W. D. Phillips, Phys. Rev. A **46**, 2668 (1992).
[42] I. Marzoli, J. I. Cirac, R. Blatt, and P. Zoller, Phys. Rev. A **49**, 2771 (1994).
[43] C. Gardiner, *Handbook of Stochastic Methods for Physics, Chemistry, and the Natural Sciences Springer Series in Synergetics* (Springer-Verlag, Berlin, 1985).
[44] N. Linke, D. Allcock, D. Szwer, C. Ballance, T. Harty, H. Janacek, D. Stacey, A. Steane, and D. Lucas, Appl. Phys. B **107**, 1175 (2012).
[45] R. J. Hendricks, J. L. Sørensen, C. Champenois, M. Knoop, and M. Drewsen, Phys. Rev. A **77**, 021401 (2008).